AGU PUBLICATIONS

JGR

Journal of Geophysical Research: Atmospheres

RESEARCH ARTICLE

10.1002/2014JD022905

Key Points:

- Test various hydrological model performances based on soil wetness conditions
- BMA-based multiple weights reflect strengths of various hydrological models
- Enhance the multimodel simulation approach in predicting soil moisture dynamics

Correspondence to:
B. P. Mohanty,
bmohanty@tamu.edu

Citation:
Kim, J., B. P. Mohanty, and Y. Shin (2015), Effective soil moisture estimate and its uncertainty using multimodel simulation based on Bayesian Model Averaging, *J. Geophys. Res. Atmos.*, *120*, doi:10.1002/2014JD022905.

Received 25 NOV 2014
Accepted 17 JUL 2015
Accepted article online 22 JUL 2015

Effective soil moisture estimate and its uncertainty using multimodel simulation based on Bayesian Model Averaging

Jonggun Kim[1], Binayak P. Mohanty[1], and Yongchul Shin[1]

[1]Department of Biological and Agricultural Engineering, Texas A&M University, College Station, Texas, USA

Abstract Various hydrological models have been developed for estimating root zone soil moisture dynamics. These models, however, incorporated their own parameterization approaches indicating that the output from the different model inherent structures might include uncertainties because we do not know which model structure is correct for describing the real system. More recently, multimodel approaches using a Bayesian Model Averaging (BMA) scheme can improve the overall predictive skill while individual models retain their own uncertainties for simulated soil moisture based on a single set of weights in modeling under different land surface wetness conditions (e.g., wet, moderately wet, and dry conditions). In order to overcome their limitations, we developed a BMA-based multimodel simulation approach based on various soil wetness conditions for estimating effective surface soil moisture dynamics (0–5 cm) and quantifying uncertainties efficiently based on the land surface wetness conditions. The newly developed approach adapts three different hydrological models (i.e., Noah Land Surface Model, Noah LSM; Soil-Water-Atmosphere-Plant, SWAP; and Community Land Model, CLM) for simulating soil moisture. These models were integrated with a modified-*micro*GA (advanced version of original Genetic Algorithm (GA)) to search for optimized soil parameters for each model. Soil moisture was simulated from the estimated soil parameters using the hydrological models in a forward mode. It was found that SWAP performed better than others during wet condition, while Noah LSM and CLM showed a good agreement with measurements during dry condition. Thus, we inferred that performance of individual models with different model structures can be different with land surface wetness. Taking into account the effects of soil wetness on different model performances, we categorized soil moisture measurements and estimated different weights for each category using the BMA scheme. Effective surface soil moisture dynamics were obtained by aggregating multiple weighted soil moisture. Our findings demonstrated that the effective soil moisture estimates derived by this approach showed a better match with the measurements compared to the original models and single-weighted outputs. Multimodel simulation approach based on land surface wetness enhances the ability to predict reliable soil moisture dynamics and reflects the strengths of different hydrological models under various soil wetness conditions.

1. Introduction

Soil moisture plays a key role in hydrologic processes such as soil water retention, infiltration, evapotranspiration, and groundwater recharge, which control water balance and land surface energy balance [*Zhu and Mohanty*, 2006; *Brocca et al.*, 2010; *Leung et al.*, 2011]. Various hydrological models have been developed and used widely for soil moisture predictions such as Noah Land Surface Model (Noah LSM) [*Ek et al.*, 2003], Soil-Water-Atmosphere-Plant (SWAP) [*Van Dam et al.*, 1997], Community Land Model (CLM) [*Oleson et al.*, 2010], Variable Infiltration Capacity [*Liang et al.*, 1994], and Mosaic Land Surface Model (Mosaic LSM) [*Koster and Suarez*, 1996], among others. The Global Land Data Assimilation Systems use these hydrological models for validating pixel-scale soil moisture from satellite platforms and evaluating water/energy cycle and fluxes near the land surface [*Liu et al.*, 2009]. The North American Land Data Assimilation System has monitored and predicted hydrological drought conditions using state variables (e.g., soil moisture dynamics, runoff, evaporation, etc.) estimated from various hydrological models [*Ek et al.*, 2011]. However, these models incorporated with their own parameterization schemes and simplified processes that might not consider adequately the real-world conditions indicating that each model has its own strengths and drawbacks for certain processes [*Hsu et al.*, 2009]. Thus, inherent model structures might produce different model outputs and cause uncertainties due to different model structures and input parameters (i.e., atmospheric forcings, soil textures, vegetation covers, initial and bottom boundary conditions, etc.).

Many stochastic techniques and methods have been developed and extended to overcome the limitations of modeling. Genetic algorithms (GAs) [*Holland*, 1975], Shuffled Complex Evolution-University of Arizona (SCE-UA) [*Duan et al*., 1992], and Particle Swarm Optimization (PSO) [*Kennedy and Eberhart*, 2001] have been applied in estimating effective model parameters. Bayesian Model Averaging (BMA) [*Hoetting et al*., 1999], Hydrological Uncertainty Processor [*Krzysztofowicz*, 1999; *Krzysztofowicz and Kelly*, 2000], Ensemble Model Output Statistics (E-MOS) [*Gneiting et al*., 2005], and Model Conditional Processor [*Todini*, 2008; *Coccia and Todini*, 2011] have been used to account for the model structural uncertainties. GAs have been used to minimize errors in searching optimized model parameters based on inversion model [*Reed et al*., 2000; *Ines and Mohanty*, 2008, 2009; *Zhang et al*., 2009; *Shin et al*., 2012; *Shin and Mohanty*, 2013; *Shin et al*., 2013]. *Zhang et al*. [2008] integrated several global optimization algorithms (i.e., GA, SCE-UA, PSO, etc.) with Soil and Water Assessment Tool and compared their performances in calibrating model input parameters. They showed that GA found better optimized model parameters than others, although a large number of computational resources were required. Further, the near-surface [*Ines and Mohanty*, 2008] and layer-specific data assimilation [*Shin et al*., 2012] approaches using GA coupled with SWAP based on inversion model were developed for quantifying effective soil hydraulic properties in the homogeneous and heterogeneous soil profiles. Their findings indicated that the estimated effective soil parameters at the near-surface and subsurface layers can be adequately conditioned by GA. However, although model parameter uncertainties for a single model can be minimized by simulation-optimization schemes (e.g., GA-SWAP, etc.), bias due to different model structures still remain (considerably) in model outputs [*Hoetting et al*., 1999; *Georgakakos et al*., 2004; *Ajami et al*., 2007].

A BMA scheme has been proposed to account for model structural uncertainties efficiently and improve their predictive capabilities of different models through a weighted average of probability density functions (PDFs) of hydrological models [*Hoetting et al*., 1999]. Currently, the technique has been applied to multiple hydrological model simulations as averaging scheme and weather prediction models to create forecast ensembles [*Raftery et al*., 2005; *Wöhling and Vrugt*, 2008; *Duan and Phillips*, 2010; *Wu et al*., 2012].

BMA usually estimates a representative weight (a single set of weights) for individual PDF of each model over the training period and then in turn aggregates different model predictions based on the estimated weights indicating how each model contributes to the predictive skill [*Ajami et al*., 2007; *Rojas et al*., 2008; *Tsai and Li*, 2008; *Zhang et al*., 2009]. However, the weighted values can vary in the model performances during the training period because some hydrological models predict better outputs during the rainy period, while others perform better under the (relatively) dry condition [*Radell and Rowe*, 2008; *Hsu et al*., 2009]. In order to overcome these limitations, recent studies adopted the sliding window algorithm to obtain the weights of individual models optimally [*Raftery et al*., 2005; *Vrugt and Robinson*, 2007]. This approach assigns different weights to the models as the window slides over the training period. However, the strengths of hydrological models may not be adequately reflected by assigning different weights to the models during the training period across time. Thus, *Duan et al*. [2007] improved the BMA scheme for stream flow predictions using an alternative way that adopts the multiple sets of weights to consider different portions of the hydrograph instead of time-based weighting schemes. None of the previous studies, however, considered an approach of soil-wetness-based weighting scheme. Such a scheme may be more suitable for identifying soil moisture variability because soil moisture predictions from different hydrological models vary based on antecedent land surface wetness conditions (i.e., wet, moderately wet, and dry conditions).

In this study, we explored a multiple-model simulation approach for estimating effective surface soil moisture dynamics (0–5 cm) and quantifying uncertainties due to different model parameters and structures. The objectives of this study are twofold: (1) to develop a BMA-based multimodel simulation approach based on the land surface wetness conditions in estimating effective soil moisture dynamics with a modified-*micro*GA (Genetic Algorithm) for soil hydraulic parameter optimization and (2) to evaluate different model parameters and structural uncertainties under different hydroclimatic conditions.

2. Methodology

2.1. Bayesian Model Averaging Based Multimodel Simulation Approach

We developed a multimodel simulation approach adapting various hydrological models based on a Bayesian Model Averaging (BMA) scheme for estimating effective surface (0–5 cm) soil moisture dynamics and

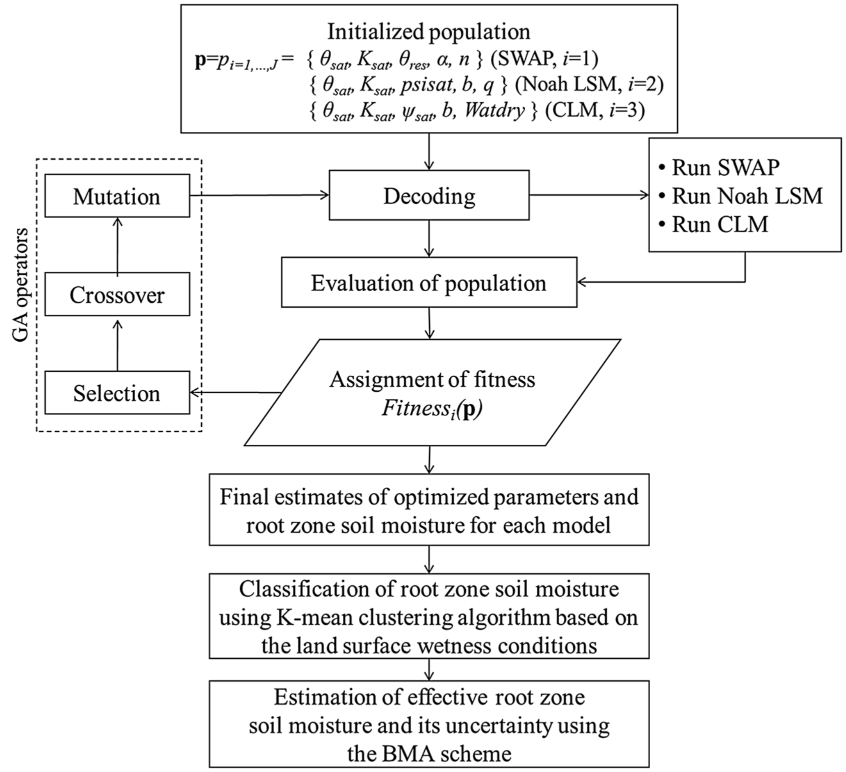

Figure 1. Schematic diagram of the Bayesian Model Average (BMA)-based multimodel simulation approach.

quantifying uncertainties due to different model parameterizations and structures. Figure 1 shows the schematic diagram of our proposed approach. In this study, we adapted three different hydrological models (i.e., Noah Land Surface Model, Noah LSM; Community Land Model, CLM; and Soil-Water-Atmosphere-Plant, SWAP) for estimating surface soil moisture dynamics reflecting their inherent strengths. Noah LSM and CLM have been used extensively in evaluating water/energy cycles and fluxes including soil moisture prediction near the land surface as the dynamic land surface component of global climate modeling (e.g., Community Earth System Model and Weather Research and Forecasting), and SWAP also has been verified and used widely for predicting crop yields and soil moisture status in various studies [*Oleson et al.*, 2008; *Hong et al.*, 2009; *Shin et al.*, 2012]. A modified-*micro*GA was integrated with these models for searching optimized parameters of each hydrological model and quantifying the model parameter uncertainty. To quantify the model structural uncertainty, we employed the BMA scheme calculating different weights of simulated results based on output fitness values of individual models. The multimodel simulation approach based on the BMA scheme was evaluated under two different hydroclimatic conditions.

2.2. Characteristics of the Hydrological Models

2.2.1. Noah Land Surface Model

The original Noah Land Surface Model (Noah LSM v2.7.1) is an advanced version of the Oregon State University land model [*Ek et al.*, 2003]. This model has been widely used in both coupled (integrated with other models) and uncoupled (stand-alone) modes for simulating water and energy fluxes at various spatial scales. In this study, we adapted the uncoupled mode as a one-dimensional (1-D), physically based model for estimating the soil moisture dynamics at field scales. Noah LSM calculates the total evapotranspiration by summing the direct evaporation from top soil layer, canopy evaporation, and potential Penman-Monteith transpiration [*Rosero et al.*, 2010]. The model has typically four soil layers with the thicknesses of 10, 30, 60, and 100 cm (total soil depth of 200 cm), but we changed top soil layer depth to 5 cm (while maintaining the same total root zone depth) to be compared to the soil moisture observation (top 5 cm) in this study. It adapts a diffusion form of the Richards' equation

Table 1. Comparison of Main Characteristics of the Three Hydrological Models

	Noah LSM	SWAP	CLM
Default thickness of top soil layer	10 cm (Total four layers)	1 cm (Total 10 layers with small compartments)	1.75 cm (Total 10 layers)
Runoff scheme	Simple Water Balance (SWB) model	Horton and Dunne Overland flow	TOPMODEL
Soil hydraulic properties	Clapp and Hornberger	van Genuchten and Mualem	Clapp and Hornberger
Surface evaporation	Penman potential evaporation	Penman-Monteith	Philip and De Vries diffusion model and BATS model
Plant system	Canopy resistance function	Linear production function and WOFOST model	Dynamic global vegetation model
Bottom boundary condition	Free drainage	Free drainage	Dynamic groundwater table (SIMGM)

(equation (1)) for soil moisture estimation. Hydraulic conductivity and soil water retention are calculated based on the *Clapp and Hornberger* [1978] equations (equations (2) and (3)),

$$\frac{\partial\theta}{\partial t}=\frac{\partial}{\partial z}\left(D(\theta)\frac{\partial\theta}{\partial z}\right)+\frac{\partial K(\theta)}{\partial z}+Q \tag{1}$$

$$\psi=\psi_{\mathrm{sat}}\left(\frac{\theta}{\theta_{\mathrm{sat}}}\right)^{-b} \tag{2}$$

$$K(\theta)=K_{\mathrm{sat}}\left(\frac{\theta}{\theta_{\mathrm{sat}}}\right)^{2b+3} \tag{3}$$

where θ is the volumetric soil water content (cm^3 cm^{-3}), z is the soil depth (cm) taken positive upward, $D(\theta)$ is the soil water diffusivity (cm^2 d^{-1}) ($K(\theta)\frac{\partial\psi}{\partial\theta}$), $K(\theta)$ is the unsaturated hydraulic conductivity (cm d^{-1}), Q is a soil moisture sink term, which is the root water extraction rate by plants, ψ and ψ_{sat} are the soil matric potential and saturated soil matric potential (cm), b is the curve fitting parameter related to the pore size distribution (−), and θ_{sat} and K_{sat} are the saturated soil moisture content (cm^3 cm^{-3}) and saturated hydraulic conductivity (cm d^{-1}), respectively.

Noah LSM has been enhanced to achieve better performance by incorporating complex canopy resistance, bare soil evaporation, surface runoff, and higher-order time integration schemes. Additional model processes and assumptions are provided in Table 1 and by *Ek et al*. [2003]. The model has been tested and showed good performance in humid and temperate hydroclimate regions [*Koren et al*., 1999; *Sridhar et al*., 2002; *Ek et al*., 2003]. However, it still has limitations in applying to arid hydroclimate regions. The limitations might be caused by its assumption that latent heat flux associated strongly with evaporation and the distribution of soil moisture content is negligible in the top soil layer when the water content is lower than the wilting point (drying season) [*Katata et al*., 2007]. Also, the thickness of top soil layer (10 cm as a default) is thicker than those of other models (i.e., SWAP and CLM), which can lead to overestimations of soil moisture [*Sahoo et al*., 2008].

2.2.2. Soil-Water-Atmosphere-Plant Model

Soil-Water-Atmosphere-Plant (SWAP) [*Van Dam et al*., 1997] has been used for simulating soil water flow between the soil, water, atmosphere, and plant system [*Agnese et al*., 2007; *Ying et al*., 2011]. This model contains physical processes for soil water flow, potential and actual evapotranspiration, crop growth, and irrigation. Daily potential evapotranspiration is estimated using the Penman-Monteith method with daily meteorological data or crop factors (i.e., minimum resistance, leaf area index, and crop height), and the actual evapotranspiration rate can be calculated using the root water uptake reduction and maximum soil evaporation flux [*Van Dam et al*., 1997] (Table 1). This model simulates soil moisture dynamics in the soil profile using the mixed form Richards' equation (equation (4)) and the soil hydraulic properties represented by the analytical expression of Mualem and van Genuchten (equations (5) and (6)) [*Mualem*, 1976; *Van Genuchten*, 1980],

$$\frac{\partial\theta}{\partial t}=\frac{\partial}{\partial z}\left[K(\psi)\left(\frac{\partial\psi}{\partial z}+1\right)\right]-Q \tag{4}$$

$$S_e=\frac{\theta(\psi)-\theta_{\mathrm{res}}}{\theta_{\mathrm{sat}}-\theta_{\mathrm{res}}}=\left[\frac{1}{1+|\alpha\psi|^n}\right]^m \tag{5}$$

$$K(\psi)=K_{\mathrm{sat}}S_e^{\lambda}\left[1-\left(1-S_e^{1/m}\right)^m\right]^2 \tag{6}$$

where n (−), m (−), λ (−), and α (cm^{-1}) are the empirical shape factors of the retention and conductivity functions, $m = 1 - 1/n$, S_e is the relative saturation (−), θ_{res} is the residual water content (cm^3 cm^{-3}), and $K(\psi)$ is the hydraulic conductivity (cm d^{-1}) at matric potential ψ.

SWAP simulates water flow, solute transport, heat flow, and crop growth simultaneously at field scales. In order to better simulate infiltration and evaporation fluxes in the vertical soil column, the soil profile (0–200 cm) was discretized in this study with finer intervals (1, 5, and 10 cm for the 1st–10th, 11th–20th, and 21st–32nd layers, respectively, except of 20 cm for the 33rd layer), especially for the soil surface (0–10 cm) where water content and pressure head gradients change sharply [*Van Dam et al.*, 1997]. However, a key limitation of the SWAP model is that it does not consider the regional groundwater hydrology and seasonal variation of boundary fluxes at the lower boundary [*Kroes et al.*, 1998]. For the detailed information about SWAP readers can refer to *Van Dam et al.* [1997].

2.2.3. Community Land Model

Community Land Model (CLM) [*Oleson et al.*, 2010] is the land surface model that provides the land surface forcing as the physical boundary for the atmospheric model in the Community Climate System Model. This model estimates bare soil evaporation based on the *Philip and de Vries* [1957] diffusion model and calculates transpiration using an aerodynamic approach of the Biosphere Atmosphere Transfer Scheme (BATS) model [*Dickinson et al.*, 1993]. Other model processes are provided in Table 1. CLM has a 10 layered soil column with the fixed thickness of 1.75, 2.76, 4.55, 7.5, 12.36, 20.38, 33.60, 55.39, 91.33, and 113.7 cm (total depth of 343 cm), and in this study averaged soil water content of the first two soil layers are used for comparison with the observations. The vertical soil water flow is solved by the modified Richards' equation (equation (7)) [*Zeng and Decker*, 2009]. This equation is derived by subtracting the hydrostatic equilibrium soil moisture distribution from the original Richards' equation for improving the mass conservative numerical scheme when the water table is within the soil column,

$$\frac{\partial \theta}{\partial t} = \frac{\partial}{\partial z}\left[K\left(\frac{\partial(\psi - \psi_e)}{\partial z}\right)\right] - Q \tag{7}$$

where ψ_e is the equilibrium soil matric potential (cm). The hydraulic conductivity is derived from equation (3), and equilibrium soil matric potential and equilibrium volumetric water content are shown in equations (8) and (9) based on *Clapp and Hornberger* [1978],

$$\psi_e = \psi_{sat}\left(\frac{\theta_e(z)}{\theta_{sat}}\right)^{-b} \tag{8}$$

$$\theta_e(z) = \theta_{sat}\left(\frac{\psi_{sat} + z_{\nabla} - z}{\psi_{sat}}\right)^{-\frac{1}{b}} \tag{9}$$

where $\theta_e(z)$ is the equilibrium (e) volumetric water content (cm^3 cm^{-3}) at depth z ($z_{\triangledown}$ is the water table depth).

In CLM, 10 soil layers discretized unevenly include a thin top soil layer (1.75 cm) needed to better simulate infiltration and evaporation fluxes [*Sahoo et al.*, 2008]. Furthermore, CLM considers the variability in ground water table as the lower boundary condition using the SIMple Groundwater Model (SIMGM) [*Niu et al.*, 2007]. A groundwater component is defined as an unconfined aquifer below the soil column (343 cm). To obtain the water table depth, the model parameterizes groundwater discharge and recharge with various constants derived from sensitive analysis [*Niu et al.*, 2007]. On the other hand, the model assumes that runoff generation is controlled by saturation area derived from topographic information and its parameterization is based on an exponential form, which is obtained from observations of the upper soil layers over small watersheds. However, this runoff generation could be also driven by the relationship between rainfall intensity and soil infiltration capacity, especially in regions with thick soils or deep groundwater. The assumption of dominant topographic control might lead to erroneous simulations for the subsurface runoff [*Li et al.*, 2011].

2.2.4. Soil Parameters of the Hydrological Models

Parameter optimization using a modified-*micro*GA was implemented to identify the soil hydraulic properties as unknown parameters whose variation has large effects on the model outputs [*Musters et al.*, 2000; *Hupet et al.*, 2002; *Ritter et al.*, 2003]. Several major input parameters related to soil moisture dynamics were selected as shown in Table 2 (Noah LSM - θ_{sat}, K_{sat}, psi_{sat} ($\partial\psi_{sat}/\partial z$), b, q; SWAP - θ_{sat}, K_{sat}, θ_{res}, α, n;

Table 2. Summary of Soil Hydraulic Parameters and its Feasible Ranges Used in the Modified-*Micro*GA for the Three Hydrological Models

LSMs	Parameters ($\mathbf{p} = p_{i=1,\ldots,J}$)	Descriptions	Unit	Min.[a]	Max.[a]	No. of Bits	Binaries (2^L)
SWAP ($i = 1$)	θ_{sat}	Saturated water contents	$cm^3\ cm^{-3}$	0.37	0.55	5	32
	K_{sat}	Saturated hydraulic conductivity	$cm\ d^{-1}$	1.84	55.70	10	1,024
	θ_{res}	Residual water contents	$cm^3\ cm^{-3}$	0.06	0.16	7	128
	α	Empirical shape parameter	cm^{-1}	0.01	0.03	5	32
	n	Empirical shape parameter	-	1.20	1.61	6	64
Noah LSM ($i = 2$)	θ_{sat}	Saturated water contents	$cm^3\ cm^{-3}$	0.35	0.55	5	32
	K_{sat}	Saturated soil hydraulic conductivity	$cm\ d^{-1}$	8.64	86.4	6	64
	psi_{sat}	Saturated soil matric potential ($\partial\psi_{sat}/\partial z$)	$cm\ cm^{-1}$	0.10	0.65	6	64
	b	Clapp-Hornberger b parameter	-	4.00	10.00	6	64
	q	Quartz content	-	0.10	0.82	5	32
CLM ($i = 3$)	θ_{sat}	Saturated water contents	$cm^3\ cm^{-3}$	0.33	0.66	5	32
	K_{sat}	Saturated soil hydraulic conductivity	$cm\ d^{-1}$	0.09	864	8	256
	ψ_{sat}	Saturated soil matric potential	cm	−75.00	−3.00	7	128
	b	Clapp-Hornberger b parameter	-	3.00	10.00	6	64
	WATDRY	Soil water content (wilting point)	-	0.02	0.30	5	32

[a]Feasible ranges of the parameters [*Liu et al.*, 2004; *Ines and Mohanty*, 2008; *Rosero et al.*, 2010].

CLM - θ_{sat}, K_{sat}, ψ_{sat}, b, *WATDRY*). Feasible ranges of the parameters (i.e., search spaces in a modified-*micro*GA) for each model were defined based on literature related to the model parameter sensitivity and to accommodate a diversity of soils ranging from clay to sandy loam [*Leij et al.*, 1999; *Liu et al.*, 2004; *Ines and Mohanty*, 2008; *Rosero et al.*, 2010; *Shin et al.*, 2012].

2.3. Modified-*Micro*GA for Estimating Optimal Parameters and Their Uncertainty

GAs are powerful algorithms based on the mechanics of nature (i.e., survival of the fittest mechanism) for searching optimal solutions from the unknown space [*Holland*, 1975]. GAs are basically composed of the GA operators such as selection, crossover, and mutation. New GA algorithms have been developed to improve the searching ability and save the computational time. *Krishnakumar* [1989] developed the so-called *micro*GA to allow more micropopulation restarts in order to overcome the relatively poor exploitation characteristic of the original GA. The micropopulation restarts searching solutions at the search space when most of the new parameter sets through the GA operator in a generation are similar up to 90%. It allowed that the GA can find solutions more efficiently saving the computational time. *Ines and Droogers* [2002] modified the *micro*GA (i.e., modified-*micro*GA) to consider interjecting new genetic materials to the micropopulation adopting a creep mutation. The creep mutation operator suggested by *Carroll* [1998] alters the parameter sets to minimize the effect of perturbation included in the converged parameter sets.

In this study, we used a modified-*micro*GA [*Ines and Droogers*, 2002] in searching the optimized soil parameters for the three selected hydrological models. The modified-*micro*GA was integrated with the hydrological models to optimize each model input parameter sets, $\mathbf{p} = \{p_{i=1,\ldots,J}\}$, as shown in Figure 1 based on the inversion model. The number of bits and binary used in the modified-*micro*GA were decided by the degree of discrete divisions between the minimum and maximum values for each parameter range (Table 2). The objective ($Z(\mathbf{p})$) functions were formulated in equation (10),

$$\text{Objective}(Z(\mathbf{p})) = \text{Minimize}\left(\frac{1}{T}\sum_{t=1}^{T}\left|\theta_{i,t}^{sim} - \theta_t^{obs}\right|\right)\forall_i \tag{10}$$

where $\theta_{i,t}^{sim}$ and θ_t^{obs} are the simulated and observed surface soil moisture, respectively.

For the parameter uncertainty analysis, we used the multipopulation with different random number seeds (−1000, −950, and −750) in the modified-*micro*GA process. After the given generations, the individual and average fitness of all the parameter sets (i.e., chromosomes) from the multiple populations were calculated. The parameter sets which have the fitness values above the average were then selected as the probable solutions. Further, we carried out the perturbation analysis in order to account for the variations of the model parameters estimating the approximated solutions ($\mathbf{p}'$) for each parameter set ($\mathbf{p}$). The perturbation analysis has been used to evaluate how variations of the model input parameters affect model outputs [*de Kroon et al.*, 1986; *Caswell*, 2000; *Benke et al.*, 2008]. The perturbed parameters were calculated as

$$\mathbf{p}' = \mathbf{p}_{\text{Avg}} \times (1 \pm x_i \xi) \tag{11}$$

where $\mathbf{p}'$ and $\mathbf{p}_{\text{Avg}}$ are the perturbed and averaged parameter set, $x_i \sim \text{Norm}(0, \sigma_i^2)$ is the normal random deviate with the mean and standard deviation calculated by the parameter sets selected (above the average fitness), ξ is the error term related to uncertain parameter (30% was applied in this study).

The surface soil moisture dynamics were simulated using the perturbed parameters, and their uncertainties with the ±95% confidence interval (PCI) were evaluated for each model.

2.4. Bayesian Model Averaging Scheme Based on the Land Surface Wetness Conditions and Model Structural Uncertainty

The BMA scheme estimates weights for various model predictions based on their probabilistic likelihood measures [*Raftery et al.*, 2005]. Here the variable "*y*" indicates the BMA prediction, namely, predictive (weighted) soil moisture and $f_{i=1,\ldots,J}$ is the individual model prediction (surface soil moisture dynamics) from the selected hydrological models ($i = 1,\ldots,J$) using the optimized parameters (section 2.3). The BMA posterior distribution of y given the model predictions can be formulated in equation (12) as follows:

$$P(y|f_1, \cdots, f_i) = \sum_{i=1}^{J} P_i(f_i|D) P_i(y|f_i, D) \tag{12}$$

where PDF ($P_i(f_i|D)$) is the posterior probability for model prediction given the training data (i.e., observations, D) and can be dealt with as weights (a single set of weights, w_i) defining the individual model's relative contributions to the BMA prediction, and J is the number of hydrological models used (i.e., 3). The conditional PDF ($P_i(y|f_i, D)$) denotes the posterior distributions of y given model prediction and observations, which is approximated by a normal distribution with mean ($\bar{f}_i$) and standard deviation (σ_i). The assumption of normal distribution could be inappropriate for soil moisture primarily driven by precipitation, while the gamma distribution is more reasonable to represent the highly skewed predictive distribution of soil moisture [*Sloughter et al.*, 2006]. However, when we tested the two assumptions (normal and gamma distribution), the assumption of normality improved more the BMA method for soil moisture prediction. In the study of *Vrugt and Robinson* [2007], they also found an improvement of BMA method with the assumption of normal distribution for streamflow forecasting instead of the gamma distribution. The posterior mean (E) and variance (Var) of the BMA prediction (y) can be computed in equations (13) and (14).

$$E\left[y|f_{i=1,\ldots,J}\right] = E\left[P\left(y|f_{i=1,\ldots,J}\right)\right] = E\left[\sum_{i=1}^{J} w_i P_i(y|f_i)\right] = \sum_{i=1}^{J} w_i f_i \tag{13}$$

$$\text{Var}\left[y|f_{i=1,\ldots,J}\right] = \sum_{i=1}^{J} w_i \left[f_i - \sum_{l=1}^{J} w_l f_l\right]^2 + \sum_{i=1}^{J} w_i \sigma_i^2 \tag{14}$$

The BMA approach then estimates the weights and variances of each simulated surface soil moisture dynamics from the three models. The variance of BMA prediction consists of the between-model variance and the within-model error variance in the BMA procedure. The values of w_i and σ^2 were estimated by the maximum likelihood (L) as described in equation (15):

$$L\left(w_{i=1,\ldots,J}, \sigma^2 | f_{i=1,\ldots,J}, y\right) = \sum_{t=1}^{T} \log\left(\sum_{i=1}^{J} w_i P_i\left(y_t | f_{i,t}\right)\right) \tag{15}$$

where T is the time domain. To find the maximum likelihood for the weights and variances, we used the DiffeRential Evolution Adaptive Metropolis-Markov Chain Monte Carlo (DREAM-MCMC) algorithm [*Vrugt et al.*, 2009]. The BMA weights are highly correlated with the model performance indicating that higher weights are assigned to a model that performed better than others. This algorithm has been used for estimating the BMA parameters (weight and variance) and is unique in solving complex, multimodel, and high-dimensional sampling problems [*Vrugt et al.*, 2008, 2009]. Thus, we estimated the weights (a single set of weights) for different hydrological models using the DREAM-MCMC algorithm and the effective surface soil moisture dynamics were calculated by aggregating the three model outputs based on the estimated weights.

Hydrological models can predict the hydrologic response well during the dry or wet season based on their own model parameters and structures [*Hsu et al.*, 2009]. In order to reflect the strengths of individual models for certain land surface wetness conditions, we categorized soil moisture measurements based on the land surface wetness conditions (e.g., wet, moderately wet, dry conditions, etc.) using the *k*-means clustering algorithm [*MacQueen*, 1967]. Near-surface soil moisture can involve several state variables of climate and physical properties (e.g., soil texture, vegetation cover, precipitation events, etc.) with respect to the wetness conditions so that the thresholds of wetness conditions can be identified using the measurements [*Narasimhan et al.*, 2005; *D'Odorico et al.*, 2007; *Brocca et al.*, 2008]. Thus, the thresholds based on the soil moisture measurements can be also applicable to other locations having similar soil type, land cover, and hydroclimatic characteristics (shown in section 3.2). The clustering algorithm determines the land surface wetness conditions based on the degree of variability between available soil moisture measurements (note that the number of wetness conditions, *G*, was manually determined). Different weights ($w_{i=1,\ldots,J}^{g=1,\ldots,G}$, multiple sets of weights) of model outputs corresponding to the land surface wetness conditions were calculated by the BMA scheme (equations (12)–(15), respectively). The estimated weights were assigned to the individual model output and then the weighted soil moisture simulations were aggregated to estimate the effective surface soil moisture dynamics reducing error due to the model structural uncertainties. In this study, we evaluated the performance of BMA scheme using a single (S-BMA) and multiple (M-BMA) sets of weights in modeling. Then, we quantified the model structural uncertainties with the ±95 PCI estimated from the posterior distribution of the BMA parameters (i.e., weight and variance).

2.5. Statistical Analysis

Three performance criteria were selected to evaluate the performance of individual model predictions and of the multiple-model simulation. They are Pearson's correlation (*R*), root-mean-square error (RMSE), and mean absolute error (MAE) as equations (16)–(18):

$$R = \frac{\sum_{t=1}^{T}\left(\theta_t^{\text{sim}} - \overline{\theta}_t^{\text{sim}}\right)\left(\theta_t^{\text{obs}} - \overline{\theta}_t^{\text{obs}}\right)}{\sqrt{\sum_{t=1}^{T}\left(\theta_t^{\text{sim}} - \overline{\theta}_t^{\text{sim}}\right)^2 \sum_{t=1}^{T}\left(\theta_t^{\text{obs}} - \overline{\theta}_t^{\text{obs}}\right)^2}} \tag{16}$$

$$\text{RMSE} = \sqrt{\frac{\sum_{t=1}^{T}\left(\theta_t^{\text{obs}} - \theta_t^{\text{sim}}\right)^2}{T}} \tag{17}$$

$$\text{MAE} = \frac{1}{T}\sum_{t=1}^{T}\left|\theta_t^{\text{obs}} - \theta_t^{\text{sim}}\right| \tag{18}$$

where $\overline{\theta}_t^{\text{sim}}$ and $\overline{\theta}_t^{\text{obs}}$ are the average of θ_t^{sim} and θ_t^{obs}, respectively.

2.6. Study Area and Description of Model Conditions

In this study, the Little Washita (LW 13) site in Oklahoma (subhumid) and Walnut Gulch (WG 82) site in Arizona (semiarid) were selected for evaluating the model parameters and structural uncertainties under two different hydroclimatic conditions (Figure 2). The LW 13 site has a subhumid climate with an average annual rainfall of approximately 750 mm with most precipitation during spring and fall. Daily mean maximum temperature is 30°C in July with annual mean temperature of 16°C. The climate of WG 82 is semiarid with an average annual rainfall of approximately 350 mm, which is mostly received from July to September. Daily mean maximum temperature of 35°C occurs in June with annual mean temperature of 17.7°C. Both study sites have a native grass cover, and their soil types are silty loam and sandy loam for LW 13 and WG 82, respectively. The three hydrological models require the common weather data (i.e., precipitation, temperature, relative humidity, solar radiation, and wind speed) and Noah LSM and CLM additionally need the air pressure values. They were collected from the USDA Agricultural Research Service

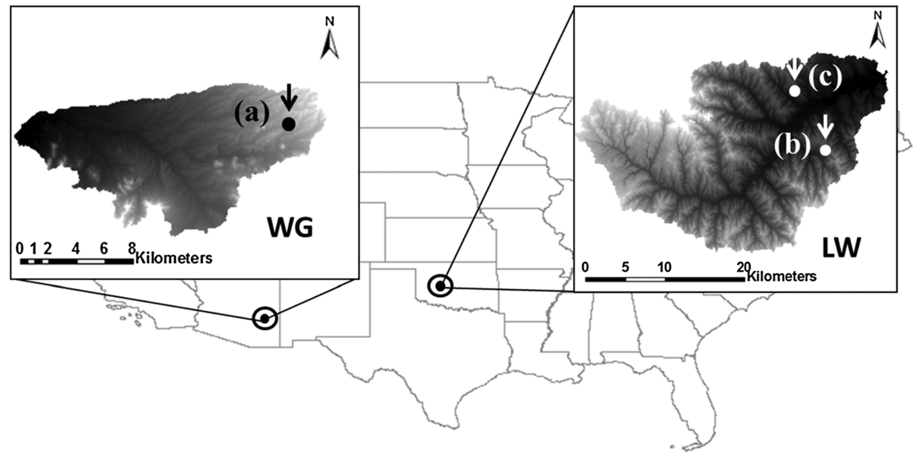

Figure 2. Study sites; (a) Walnut Gulch (WG) 82 in Arizona, (b) Little Washita (LW) 13, and (c) SCAN 2023 in Oklahoma.

(ARS 136) Micronet and the Oklahoma Mesonet weather stations (Ninnekah station) from 1 January to 31 December 1997 for the LW 13 site. The weather data sets for the WG 82 site were obtained from the Arizona Meteorological Network [*Keefer et al.*, 2009] and the Soil Climate Analysis Network (SCAN, Walnut Gulch #1) sites from 1 January to 31 December 2004.

We validated our approach with the in situ soil moisture measurements (0–5 cm) during the Southern Great Plains experiment 1997 (SGP97, day of year (DOY): 170–197) [*Mohanty and Skaggs*, 2001; *Mohanty et al.*, 2002] for the LW 13 site and Soil Moisture Experiment 2004 (SMEX04, DOY: 216–238) [*Jackson et al.*, 2009] for the WG 82 site. Here, we calibrated the multimodel approach using the measurements during the simulation periods (DOY: 170–183 for LW 13 and DOY: 216–227 for WG 82), and the validations were conducted in the given periods (DOY: 184–197 for LW 13 and DOY: 228–238 for WG 82), respectively. These experiment data sets have been validated significantly and used widely in various studies, but the experiment periods are limited. Thus, we also tested our approach using longer data sets (1 April to 31 December 2011) measured at USDA-SCAN 2023 site (Figure 2) in Little Washita watershed, in the close proximity of LW 13. The site is close to the LW 13 site having the same climate condition (subhumid) and has a grass cover and silty clay soil. The weather data sets were collected from the SCAN 2023 site from 1 January to 31 December 2011.

In order to reflect the impacts of various land surface wetness conditions in modeling as mentioned above, in situ measurements were categorized using the *k*-means clustering algorithm at the LW 13 and WG 82 sites. Thresholds of the clustering ranges could be different with site conditions such as hydroclimates due to the different climate forcing and hydrologic responses which can influence the model performance. In order to determine the appropriate range of weight sets we tested several different weight sets (e.g., 2, 3, and 4 sets) clustered using *k*-means algorithm for each site. Comparing the BMA predictions of each set to the measurements including at least 5 data in each class, we found the suitable sets of weights representing the highest correlation and reflecting the models' characteristics properly discussed in section 2.2. The in situ data were then clustered into the three ($G = 3$: wet, moderately wet, and dry conditions) and two ($G = 2$: wet and dry conditions) classes for the LW (13 and SCAN 2023), and WG (82) sites, respectively.

Various hydrological models have different initial and bottom boundary conditions due to their own structural characteristics. In the study sites, actual groundwater table is not available during the experiment periods, so we assumed that the bottom boundary condition is defined with free drainage at 2 m depths from the soil surface for the Noah LSM and SWAP models, while the bottom boundary condition for CLM was decided with the water table dynamics calculated from aquifer water storage via the SIMGM [*Niu et al.*, 2007] after spinning up the model. For the initial condition, the Noah LSM and CLM models performed a spinning up to initialize the soil profile. A uniform initial soil water pressure head distributions ($h(z,t = 0) = -100$ and -500 cm for the LW (13 and SCAN 2023) and WG (82) sites indicating the shallow/deep groundwater levels, respectively) were used for the SWAP model.

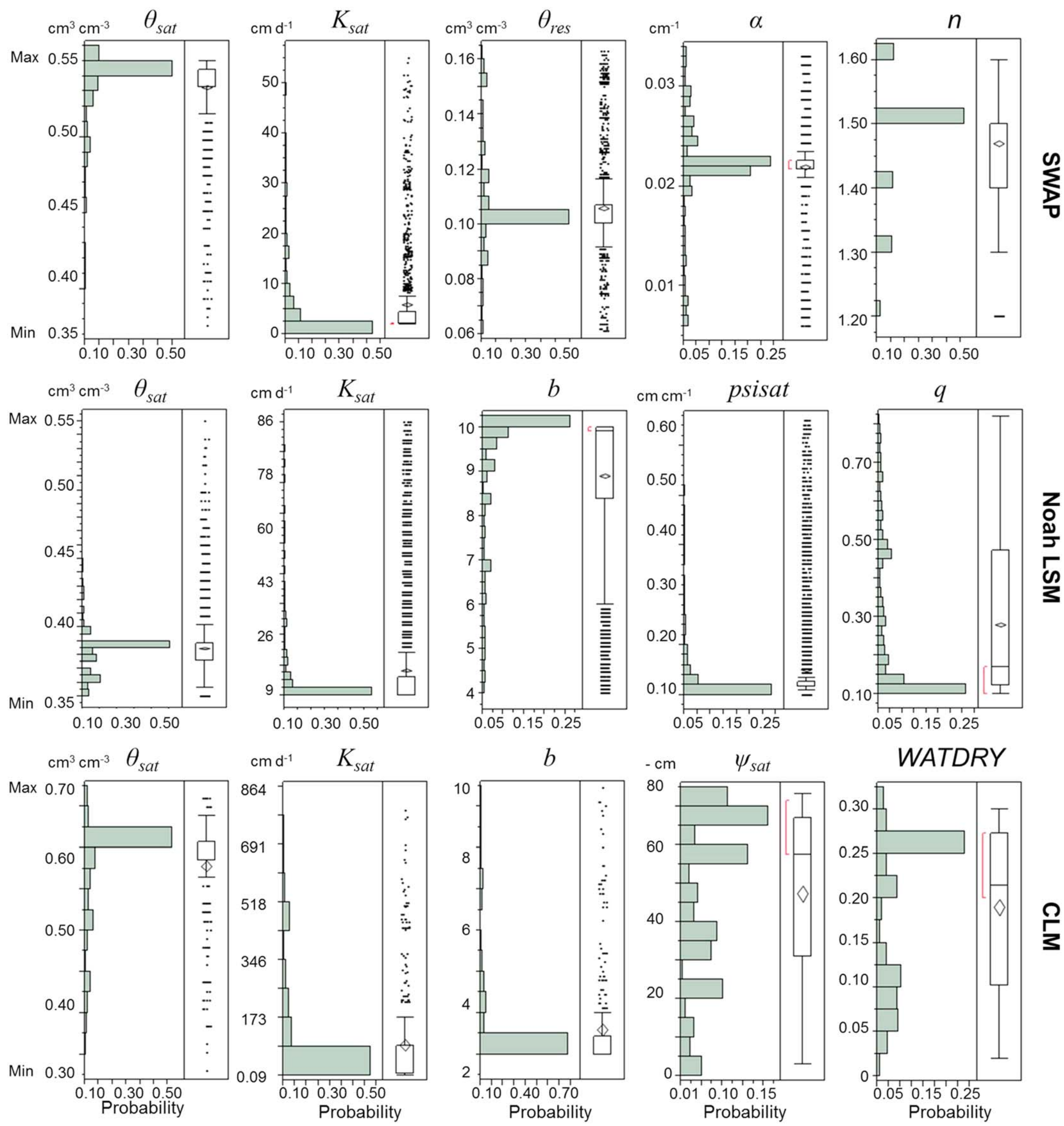

Figure 3. Probability distributions and quantile box plots of the searched soil parameters of the three hydrological models using the multiple random number seeds (i.e., −1000, −950, and −750) for the LW 13 site.

3. Results and Discussions

3.1. Estimation of Optimized Model Parameters and Their Uncertainties

The optimized model parameters and the uncertainties of each model were estimated using the modified-*micro*GA under two different hydroclimatic regions. Figure 3 shows the probability distributions and their quantile box charts for the estimated soil hydraulic parameters of each model using multiple random number seeds (i.e., −1000, −950, and −750) at the LW 13 site during the calibration period (DOY: 170–183, 1997). The estimated parameters for individual models showed the unimodal distributions indicating a probable optimized parameter value. Further, some of the parameters represented discontinuous distributions because the modified-*micro*GA searched for the possible parameter sets from the multipopulation and different random number seeds exploring the complete search space. The optimized values for each model were used for evaluating the model parameter uncertainty, estimating the effective soil moisture dynamics for the study site. Based on these results, we found that the optimized soil hydraulic parameters (θ_{sat}, b, ψ_{sat}, and K_{sat}) and their ranges (i.e., search spaces) for the three models showed differences under the same modeling conditions (i.e., atmospheric forcings, soils, vegetations, etc.). The

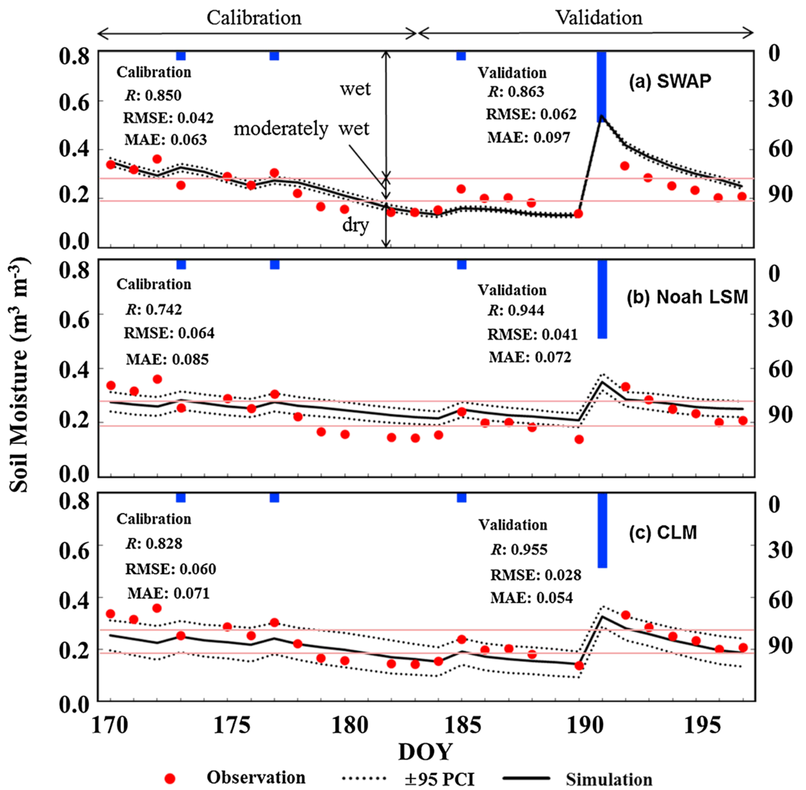

Figure 4. In situ and simulated surface soil moisture (0–5 cm) dynamics using the optimized soil parameters derived by the modified-*micro*GA for (a) SWAP, (b) Noah LSM, and (c) CLM at the LW 13 site during calibration and validation periods.

discrepancy between the models may be attributed to different parameterizations and structures that can also provide different model performances.

In order to quantify parameter uncertainties of each model, we generated 10 perturbed parameter ensembles using the statistics (mean and standard deviation) of estimated parameters based on the multiple populations and random number seeds. Then, the surface (0–5 cm) soil moisture dynamics were simulated using the perturbed parameter ensembles for each model in a forward mode. Figures 4a–4c present the comparison of in situ and simulated surface soil moisture dynamics and their uncertainty band for SWAP, Noah LSM, and CLM during the calibration and validation periods. The results showed very narrow uncertainty boundaries, because the possible parameter sets searched by the modified-*micro*GA using the different populations were very similar for the cases of SWAP and Noah LSM (Figures 4a and 4b). Some observations deviated from the narrow boundaries of the simulated soil moisture from SWAP and Noah LSM. It can be inferred that the single model could not predict properly for a certain period due to their model structural error. Overall, however, three different models predicted the surface soil moisture dynamics well in comparison with the measurements (R: 0.742–0.850, RMSE: 0.042–0.064, and MAE: 0.063–0.085 during the calibration period; R: 0.863–0.955, RMSE: 0.028–0.062, MAE: 0.054–0.097 during the validation period). The SWAP model showed better performance than others at the LW 13 site during the calibration period, while CLM performed better during the validation period. On a closer view, the simulated surface soil moisture dynamics by SWAP matched well with the measurements during DOY 170–177 (volumetric water content above 0.280 $m^3\,m^{-3}$), but the CLM results were identified better during DOY 177–190 (volumetric water content below 0.190 $m^3\,m^{-3}$). Also, both Noah LSM and CLM performed well during DOY 192–197 (for volumetric water content 0.190–0.280 $m^3\,m^{-3}$). The simulated surface soil moisture from SWAP was more sensitive to the precipitation which can be associated directly with the wet surface condition, compared to those of Noah-LSM and CLM, because of a thin top soil layer (1 cm) which can capture the dynamic change of surface soil moisture. Thus, it showed rather good agreement with measurements than other models during wet condition (Figure 4a). In contrast, CLM showed poor performance during

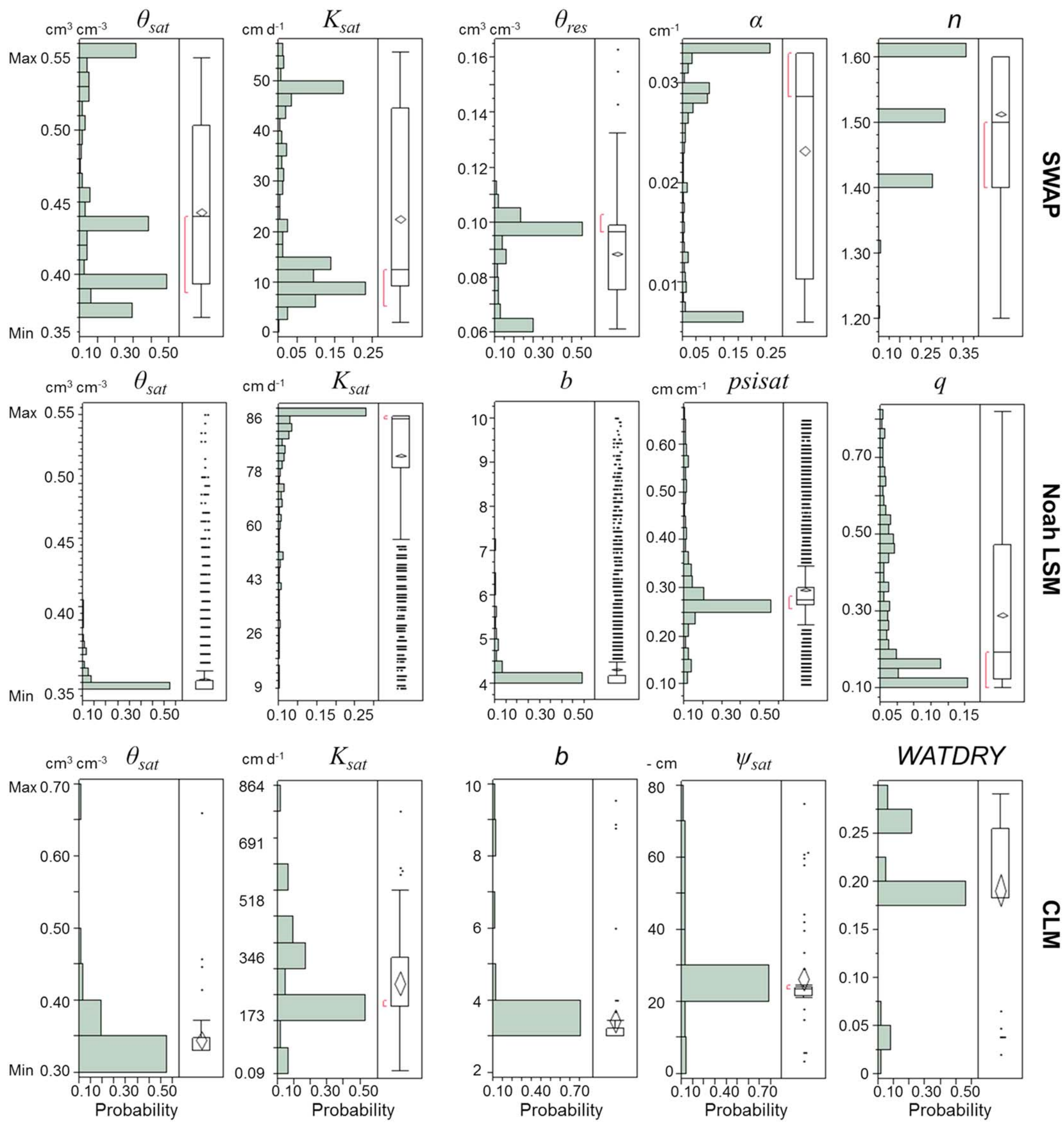

Figure 5. Probability distributions and quantile box plots of the searched soil parameters of the three hydrological models using the multiple random number seeds (i.e., −1000, −950, and −750) for the WG 82 site.

wet condition (Figure 4c). In CLM, the simulated surface soil moisture was underestimated due to the unreliable surface runoff generation (see section 2.2.3) and high sensitivity of evaporation to precipitation. During the dry condition, CLM predicted the surface soil moisture well whereas Noah LSM somewhat overestimated the surface soil moisture. This may be attributed to the layer thickness of the models. The thicker top layer of Noah LSM holds more soil water after precipitation events than the thin soil layers of the other models (Figure 4b). These findings support those of *Hsu et al.* [2009] as they state that the performances of different models has their own strengths and weaknesses for certain processes, and we found that the performances of different hydrological models (Noah LSM, CLM, and SWAP) might vary based on the different land surface wetness conditions (e.g., wet, moderately wet, and dry conditions).

Figure 5 shows the probability distributions of estimated effective soil hydraulic parameters based on the multiple random number seeds for the WG 82 site during the calibration period (DOY: 216–227, 2004). Most of the probability distributions were unimodal for the Noah LSM and CLM parameters, except q (in Noah LSM) and *WATDRY* (in CLM) variables. However, the model parameter distributions of SWAP have multiple modes indicating local minima that can be derived by the modified-*micro*GA in the search space.

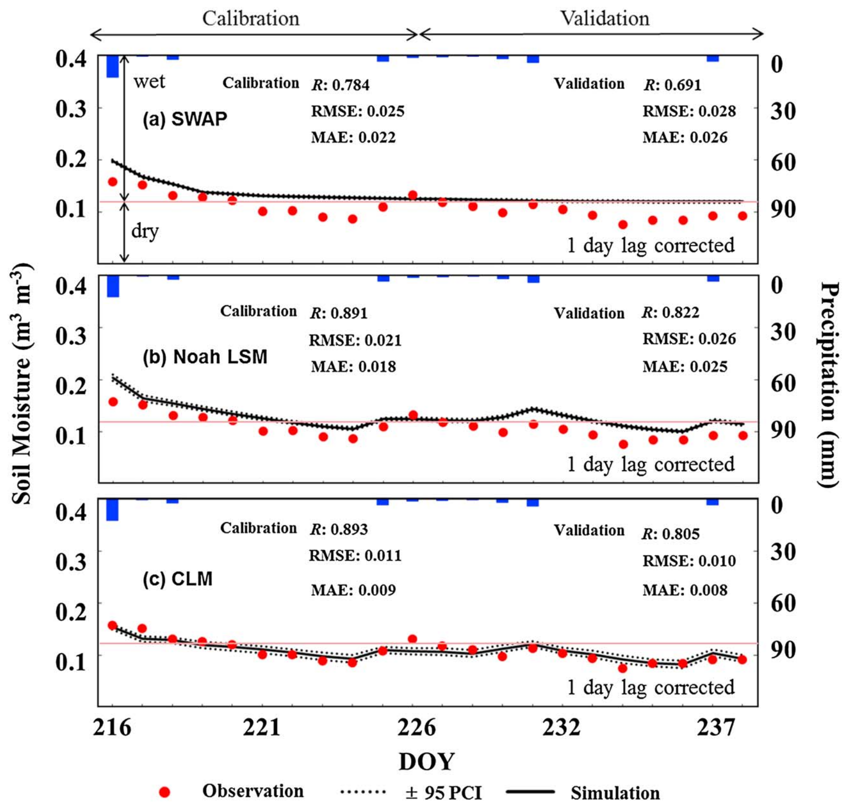

Figure 6. In situ and simulated surface soil moisture (0–5 cm) dynamics using the optimized soil parameters derived by the modified-*micro*GA for (a) SWAP, (b) Noah LSM, and (c) CLM at the WG 82 site during calibration and validation periods.

Thus, the local minima that were significantly deviated from the referenced parameter ranges (UNSODA [*Leij et al*., 1999], Soil Survey [*Wösten et al*., 1994], Rosetta [*Schaap et al*., 1999], and Clapp and Hornberger table [*Clapp and Hornberger*, 1978]) of the sandy loam soil type (predominant at the WG 82 site) were excluded. Also, we found a response time lag of 1 day between observed precipitation and simulated soil moisture that could be attributed to the difference of actual measurement time during the day and model time steps (starting at 12 midnight) at the WG 82 site. Figures 6a–6c show the comparison of measured and simulated surface soil moisture dynamics with ±95 PCI after a 1 day lag was corrected. The simulated soil moisture dynamics from the three models agreed well with the measurements. Statistical analyses demonstrated that CLM performed better than others during the calibration and validation period as shown in the figures. The outputs of SWAP showed more uncertainties compared to the results of the other two models under the prevailing condition (e.g., relatively small precipitation and high solar radiation) as shown in Figure 6 (DOY: 222–238). SWAP tends to overestimate the surface soil moisture when the soil is relatively dry along with small precipitation and high evapotranspiration rate estimated using Penman-Monteith method [*Baroni and Tarantola*, 2012]. We also found that the SWAP results matched the measurements during DOY 216–221 (above 0.125 $m^3 m^{-3}$, wet condition) with higher correlation ($R = 0.945$) than others ($R = 0.911$ for Noah LSM and $R = 0.889$ for CLM) at the WG 82, while the CLM model identified better during the period of DOY 222–238 (below 0.125 $m^3 m^{-3}$, dry condition). In general, CLM showed a good performance for this site considering the water table dynamics as a bottom boundary condition, but the model underestimated the surface soil moisture during wet condition that can be associated to more moisture loss through evaporation. Noah LSM appeared to somewhat overestimate the surface soil moisture because of the thick top soil layer, but the model showed a similar tendency as CLM compared to the field observations (Figure 6b). Compared to the results at LW 13, the parameter uncertainty boundaries of each model were smaller, because of the low variability of surface soil moisture estimations. It may indicate that the relatively low rainfall amounts at the WG 82 site (semiarid) cause the low-surface soil moisture variability in modeling.

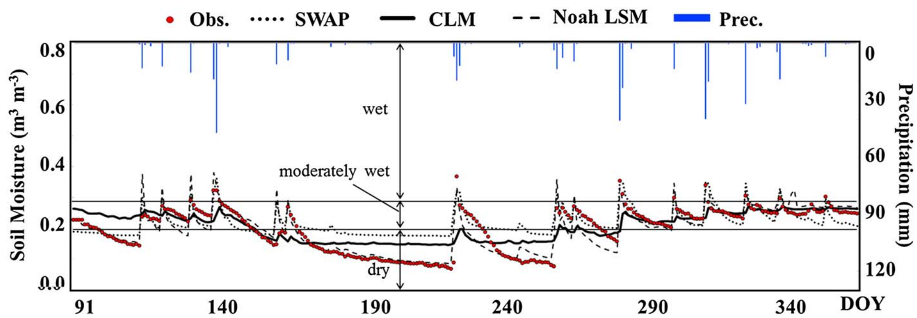

Figure 7. In situ and simulated surface soil moisture (0–5 cm) dynamics using the optimized soil parameters derived by the modified-*micro*GA for SWAP, Noah LSM, and CLM at the SCAN 2023 site.

For the longer period simulation at SCAN 2023 site, the three models integrated with the modified-*micro*GA predicted the surface soil moisture well representing a good agreement with the measurements (R: 0.75, RMSE: 0.052, and MAE: 0.039 for SWAP; R: 0.89, RMSE: 0.033, and MAE: 0.023 for Noah LSM; R: 0.78, RMSE: 0.046, and MAE: 0.035 for CLM). Yet the predictions from the models indicated different trends under the different land surface wetness conditions defined with the same thresholds of the LW 13 site (Figure 7). SWAP shows good response to precipitation events in predicting the surface soil moisture peaks better than others during the wet condition, whereas the simulated surface soil moisture decreased rapidly during the dry-down phase (i.e., moderately wet and dry conditions) after the precipitation event. On the other hand, CLM and Noah LSM showed best performances in moderately wet and dry conditions, respectively. Evaporation in CLM is very sensitive to the precipitation on short time scale (the case of LW 13) so that the evaporation removes soil water from the top soil layer. This is the reason why CLM predicted well the low-surface soil moisture during dry condition at the LW 13 site. In contrast, on long time scale, more soil water can be retained from previous precipitation events that may cause the overestimation of surface soil moisture.

Overall, the predicted surface soil moisture dynamics using the three models based on the optimized parameters derived by the modified-*micro*GA matched well with the measurements in two different hydroclimatic regions. However, the measured soil moisture dynamics could not be captured adequately by the parameter uncertainty boundaries of SWAP and Noah LSM. Furthermore, the performances of different hydrological models in estimating the surface soil moisture showed different trends under various wetness conditions and different hydroclimatic conditions. It infers that uncertainties due to the different model structures are reflected significantly in model outputs.

3.2. Estimation of Effective Surface Soil Moisture and Its Uncertainty

In order to reduce bias due to model structural uncertainties (i.e., different model parameterizations, governing equations, etc.) mentioned above, we assigned a single (S-BMA) and multiple (M-BMA) sets of weights derived by the BMA scheme to the individual surface soil moisture predictions. A single set of weight ($w_{i=1,\ldots,J}$) was estimated based on the simulation results from the three models for the LW 13 site

Table 3. A Single and Multiple Sets of the Bayesian Model Average (BMA) Weights for the Three Hydrological Models at the LW 13 Site

		Weights		
BMA set		SWAP ($i=1$)	Noah LSM ($i=2$)	CLM ($i=3$)
S-BMA[a] ($w_{i=1,\ldots,J}$)		0.291	0.005	0.704
M-BMA[b] ($w_{i=1,\ldots,J}^{g=1,\ldots,G}$)[c]	$g=1$	0.533	0.466	0.001
	$g=2$	0.001	0.293	0.706
	$g=3$	0.008	0.002	0.990

[a]S-BMA means a single set of the weights for the three models ($i=1, 2, 3$).
[b]M-BMA means multiple sets of the weights corresponding to three land surface wetness conditions ($g=1, 2, 3$ represent the wet, moderately wet, and dry conditions, respectively).
[c]Note that G and J are the number of land surface wetness conditions and hydrological models, respectively.

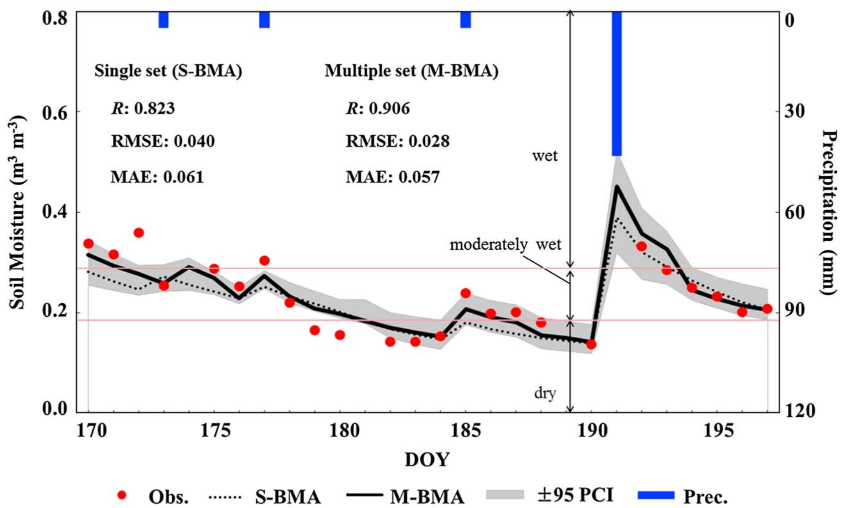

Figure 8. In situ and simulated surface soil moisture using a single (S-BMA, dotted line) and multiple (M-BMA, black line) sets of the BMA weights and ±95 PCI at the LW 13 site.

during the whole simulation period as shown in Table 3. The highest weight (0.704) was assigned to CLM, which showed the best model performance (*R*: 0.837, RMSE: 0.047, MAE: 0.036) over the simulation period, while SWAP (*R*: 0.789, RMSE: 0.053, MAE: 0.044) and Noah LSM (*R*: 0.806, RMSE: 0.054, MAE: 0.046) had relatively lower weights of 0.291 and 0.005, respectively. The aggregated surface soil moisture dynamics using a single set of weights (*R*: 0.823, RMSE: 0.040, and MAE: 0.061) for the three models matched better with the measurements than SWAP and Noah LSM predictions in Figure 8. However, there was no significant improvement of the single-weighted prediction compared to CLM prediction. This was because the single-weighted based surface soil moisture dynamics were considerably biased toward the CLM results assigned with the highest weight uniformly along the whole period and did not reflect a good performance of other models during a certain condition (e.g., wet and moderately wet). As shown in Figure 4, the SWAP model performed better during DOY 170–177 (defined as the wet condition), while Noah LSM and CLM predicted the surface soil moisture estimates better under the moderately wet and dry conditions, representing the advantages and disadvantages of each model structure. These findings demonstrated that we need to classify the simulation period for assigning different weights to the model predictions based on the land surface wetness conditions. For these reasons, we categorized the in situ measurements using the *k*-means clustering algorithm as the wet (above 0.280 $m^3\ m^{-3}$), moderately wet (0.190–0.280 $m^3\ m^{-3}$), and dry (below 0.190 $m^3\ m^{-3}$) conditions, respectively. Then, we estimated multiple sets of the weight (i.e., $w^{g=1}_{i=1,\ldots,J}$-wet, $w^{g=2}_{i=1,\ldots,J}$-moderately wet, and $w^{g=3}_{i=1,\ldots,J}$-dry conditions) based on the categorized soil moisture measurements for the LW 13 site (see Table 3). The highest weight (0.533) was assigned to the SWAP results during the wet condition at the LW 13 site, while CLM had the highest weights (0.706 and 0.990) during the moderately wet and dry conditions, respectively. These multiple-weight values can be seen as the performance of individual models based on the advantages of each model structure. The

Table 4. Single and Multiple Sets of the Bayesian Model Average (BMA) Weights for the Three Hydrological Models at the WG 82 Site

		Weights		
BMA Set		SWAP ($i = 1$)	Noah LSM ($i = 2$)	CLM ($i = 3$)
S-BMA[a] ($w_{i=1,\ldots,J}$)		0.001	0.053	0.946
M-BMA[b] ($w^{g=1,\ldots,G}_{i=1,\ldots,J}$)[c]	$g = 1$	0.936	0.001	0.063
	$g = 2$	0.002	0.002	0.996

[a]S-BMA means a single set of the weights for the three models ($i = 1, 2, 3$).
[b]M-BMA means multiple sets of the weights corresponding to two land surface wetness conditions ($g = 1, 2$ represent the wet and dry conditions, respectively).
[c]Note that *G* and *J* are the number of land surface wetness conditions and hydrological models, respectively.

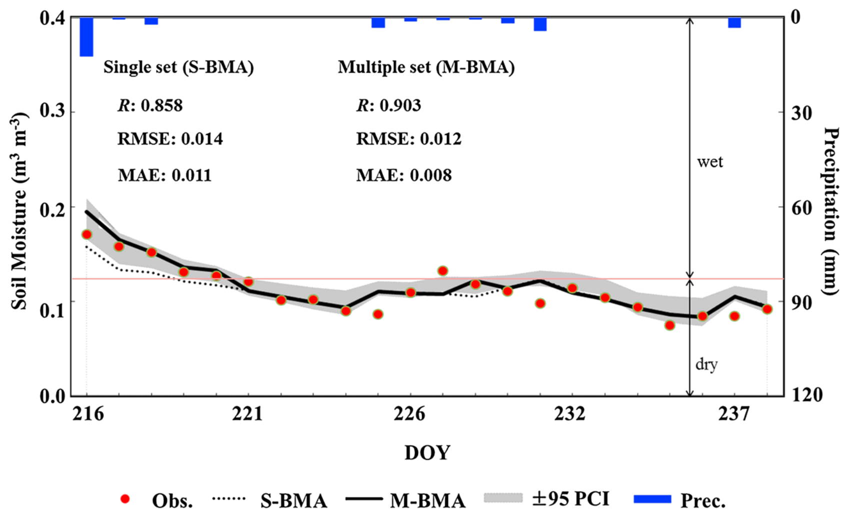

Figure 9. In situ and simulated surface soil moisture using a single (S-BMA, dotted line) and multiple (M-BMA, black line) sets of the BMA weights and ±95 PCI at the WG 82 site.

effective (multiple-weighted) surface soil moisture dynamics showed a better match with the measurements (R: 0.906, RMSE: 0.028, and MAE: 0.057) in Figure 8. Compared to the single-weighted results (Figure 8), the BMA scheme based on the multiple sets of weight (based on wetness thresholds) also improved the surface soil moisture estimations and their uncertainties, especially on DOY 170–177. Thus, our findings demonstrated that the BMA-based multimodel simulation approach with multiple sets of weights is more suitable for addressing model structural uncertainties than those with a single set of weights.

We estimated a single set of weights ($w_{i=1,\ldots,J}$) for the whole simulation period for the WG 82 site as shown in Table 4. The highest weight value (0.946) was assigned to the CLM results that show the best prediction (R: 0.856, RMSE: 0.014, and MAE: 0.011), and then in turn the low weights of 0.001 and 0.053 were assigned to SWAP and Noah LSM, respectively. The aggregated (single-weighted) surface soil moisture dynamics agreed with the measurements, but they were also biased to the CLM results representing that the predictions have uncertainties during the wet period (DOY 216–221, Figure 9) as shown in the results of LW 13 site. Thus, we categorized the simulation period into the two classes (i.e., wet and dry conditions) and estimated the two sets of the weight ($w^{g=1}_{i=1,\ldots,J}$-wet and $w^{g=2}_{i=1,\ldots,J}$-dry conditions, see Table 4) for the WG 82 site. As shown in the previous section, the simulated surface soil moisture dynamics from the SWAP model were closer to the measurements during the wet condition, while CLM performed better along the dry period. Thus, the highest weight values (0.936 and 0.996 for the wet and dry conditions) were assigned to the results of SWAP and CLM models, respectively. The aggregated surface soil moisture dynamics using multiple sets of weights (R: 0.903, RMSE: 0.012, and MAE: 0.008) identified better with the measurements than the individual models and single-weighted results. Further, a poor performance due

Table 5. Single and Multiple Sets of the Bayesian Model Average (BMA) Weights for the Three Hydrological Models at the SCAN 2023 Site

		Weights		
BMA Set		SWAP ($i=1$)	Noah LSM ($i=2$)	CLM ($i=3$)
S-BMA[a] ($w_{i=1,\ldots,J}$)		0.204	0.650	0.146
M-BMA[b] ($w^{g=1,\ldots,G}_{i=1,\ldots,J}$)[c]	$g=1$	0.592	0.406	0.002
	$g=2$	0.432	0.125	0.443
	$g=3$	0.001	0.934	0.065

[a]S-BMA means a single set of the weights for the three models ($i=1, 2, 3$).
[b]M-BMA means multiple sets of the weights corresponding to three land surface wetness conditions ($g=1, 2, 3$ represent the wet, moderately wet, and dry conditions, respectively).
[c]Note that G and J are the number of land surface wetness conditions and hydrological models, respectively.

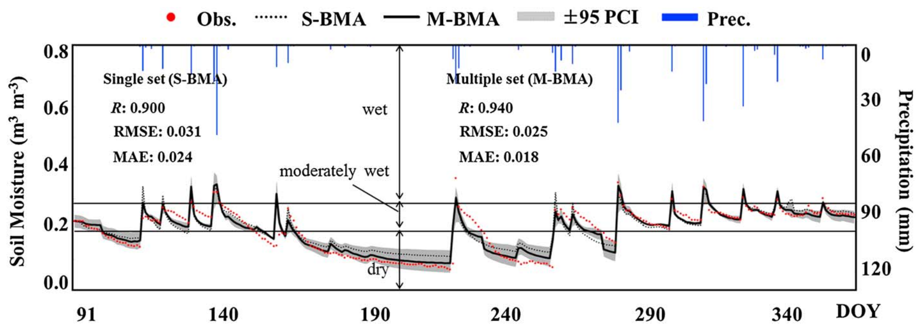

Figure 10. In situ and simulated surface soil moisture using a single (S-BMA, dotted line) and multiple (M-BMA, black line) sets of the BMA weights and ±95 PCI at the SCAN 2023 site.

to the structural errors of single model could be compensated by good performances of other models indicating that the measured soil moisture data were mostly located within the ±95 PCI.

We also tested our proposed approach using long-period data (DOY 91–365) at SCAN 2023 site. The long-period soil moisture measurements were categorized into the three classes (wet, moderately wet, and dry conditions) by the same range of the wetness conditions for LW 13, and multiple sets of weights were estimated using the BMA scheme (Table 5). The highest weights were assigned to SWAP (0.592 for wet condition), CLM (0.443 for moderately wet), and Noah LSM (0.934 for dry condition), respectively. The surface soil moisture prediction based on the multiple sets of weights showed better improvement (R: 0.940, RMSE: 0.025, and MAE: 0.018) compared to the individual model performances and single-weighted prediction (Figure 10).

Based on these findings, we suggest that model structural uncertainties can be addressed by the BMA-based multimodel simulation approach using multiple sets of weight corresponding to soil wetness conditions for the two different study sites.

4. Summary and Conclusions

Soil moisture dynamics estimated by different hydrological models are affected by their own model parameters and structures. Without identifying these uncertainties, the robustness of model outputs from various hydrological models may be elusive. Our study was focused on improving parameter and structural uncertainties caused by different hydrological models in predicting surface soil moisture. In this study, we adapted three different hydrological models (i.e., Noah LSM, SWAP, and CLM) for estimating surface (0–5 cm) soil moisture integrated with a modified-*micro*GA (advanced version of original genetic algorithm (GA)) to search optimized model parameters for each model. Here we simulated the surface soil moisture dynamics using the optimized soil parameters of each model in a forward mode. In order to address the effects of model structural uncertainties, we applied a Bayesian Model Averaging (BMA) scheme to the multimodel outputs based on the land surface wetness conditions. By aggregating the weighted model outputs for each model, the newly developed approach estimates the effective surface soil moisture dynamics and quantifies model parameter and structural uncertainties. To test our approach, we selected the Little Washita (LW 13 and SCAN 2023) in Oklahoma (subhumid) and Walnut Gulch (WG 82) in Arizona (semiarid) sites under the two different hydroclimatic conditions.

For the uncertainty analysis of soil parameters, we used the multipopulation for the modified-*micro*GA process with different random number seeds (−1000, −950, and −750). Overall, the estimated parameter distributions for individual models at the LW 13 and WG 82 sites were unimodal, which represent the optimized soil hydraulic parameters. However, the (common) optimized parameters of the three different models at the study sites had variations under the similar modeling conditions (i.e., atmospheric forcings, soils, vegetations, etc.) indicating that the individual model performances were affected by their own model parameterization and structural uncertainties.

We derived the surface soil moisture dynamics from the estimated soil parameters using the three models. Mostly, the simulated results of each model matched well with the measurements, but the SWAP and Noah LSM results still had uncertainties showing that a few soil moisture measurements were out of the uncertainty bounds at the LW 13 and WG 82 sites. Furthermore, the outputs from the three hydrological models showed different model performances under the land surface wetness (i.e., wet, moderately dry, and dry) conditions depending on their inherent model structures. In general, the SWAP model performed better than other models during the wet condition, while CLM and Noah LSM predicted better during the dry period. Thus, we applied the BMA scheme to assign single or multiple sets (corresponding to various land surface wetness conditions) of weights to each model output for the two study sites. The results showed that the effective surface soil moisture estimates based on multiple sets of weights were more identifiable with the measurements compared to both the original model and single-weighted outputs. It suggests that each model's limitations under certain wetness conditions or hydroclimatic conditions can be compensated by other model strengths. Based on these findings, our proposed methodology can be useful for predicting the effective surface soil moisture estimates and better addressing model parameter and structural uncertainties in soil moisture modeling. Further, this multimodel simulation approach will be applicable to other locations for forecasting soil moisture dynamics effectively using multiple sets of weights derived properly based on wetness conditions or several climate and physical properties.

Acknowledgments
This research was funded by NASA THP-NNX09AK73G and NSF DMS-09-34837 grants. Soil moisture data sets used in this study were collected from Southern Great Plains experiment 1997 (SGP97, contact with Michael H. Cosh at USDA-ARS Hydrology and Remote Sensing Lab), Soil Moisture Experiment 2004 (SMEX04, http://nsidc.org/data/amsr_validation/soil_moisture/smex04/index.html), and Soil Climate Analysis Network (SCAN, http://www.wcc.nrcs.usda.gov/scan/). Weather data sets were obtained from USDA Agricultural Research Service (ARS) Micronet (http://ars.mesonet.org/webrequest/), Oklahoma Mesonet stations (http://www.mesonet.org/index.php), Arizona Meteorological Network (http://ag.arizona.edu/azmet/), and Soil Climate Analysis Network (SCAN). Three hydrological models (SWAP, Noah LSM, and CLM) used in this study are available on the links as follows: SWAP (http://www.swap.alterra.nl/), Noah LSM (http://www.ral.ucar.edu/research/land/technology/lsm.php), and CLM (http://www.cesm.ucar.edu/models/clm/).

References

Agnese, C., F. Blanda, A. Drago, M. Iovino, M. Minacapilli, G. Provenzano, G. Rallo, and M. Sciortino (2007), Assessing the agro-hydrological SWAP model to simulate soil water balance in typical Mediterranean crops, *Geophys. Res. Abstr.*, *9*, 08146.

Ajami, N. K., Q. Y. Duan, and S. Sorooshian (2007), An integrated hydrologic Bayesian multimodel combination framework: Confronting input, parameter, and model structural uncertainty in hydrologic prediction, *Water Resour. Res.*, *43*, W01403, doi:10.1029/2005WR004745.

Baroni, G., and S. Tarantola (2012), A general probabilistic framework for uncertainty and sensitivity analysis of deterministic models, International Environmental Modelling and Software Society (iEMSs), 2012 International Congress on Environmental Modelling and Software Managing Resources of a Limited Planet, Sixth Biennial Meeting, Leipzig, Germany.

Benke, K. K., K. E. Lowell, and A. J. Hamilton (2008), Parameter uncertainty, sensitivity analysis and prediction error in a water-balance hydrological model, *Math. Comput. Model.*, *47*, 1134–1149.

Brocca, L., F. Melone, and T. Moramarco (2008), On the estimation of antecedent wetness conditions in rainfall-runoff modelling, *Hydrol. Processes.*, *22*, 629–642, doi:10.1002/hyp.6629.

Brocca, L., F. Melone, T. Moramarco, and R. Morbidelli (2010), Spatial-temporal variability of soil moisture and its estimation across scales, *Water Resour. Res.*, *46*, W02516, doi:10.1029/2009WR008016.

Carroll, D. L. (1998), GA Fortran driver version 1.7. [Available at http://www.cuaerospace.com/carroll/ga.html.]

Caswell, H. (2000), Prospective and retrospective perturbation analyses: Their roles in conservation biology, *Ecology*, *81*, 619–627.

Clapp, R. B., and G. M. Hornberger (1978), Empirical equations for some soil hydraulic properties, *Water Resour. Res.*, *14*(4), 601–604, doi:10.1029/WR014i004p00601.

Coccia, G., and E. Todini (2011), Recent developments in predictive uncertainty assessment based on the model conditional processor approach, *Hydrol. Earth Syst. Sci.*, *15*(10), 3253–3274.

de Kroon, H., A. Plaisier, J. van Groenendael, and H. Caswell (1986), Elasticity: The relative contribution of demographic parameters to population growth rate, *Ecology*, *67*, 1427–1431.

Dickinson, R. E., A. Henderson-Sellers, and P. J. Kennedy (1993), Biosphere atmosphere transfer scheme (BATS) version 1e as coupled to the NCAR Community Climate Model, *NCAR Tech. Note NCAR/TN-378+STR*, Natl. Cent. for Atmos. Res., Boulder, Colo.

D'Odorico, P., K. Caylor, G. S. Okin, and T. M. Scanlon (2007), On soil moisture-vegetation feedbacks and their possible effects on the dynamics of dryland ecosystem, *J. Geophys. Res.*, *112*, G04010, doi:10.1029/2006JG000379.

Duan, Q., and T. J. Phillips (2010), Bayesian estimation of local signal and noise in multimodel simulations of climate change, *J. Geophys. Res.*, *115*, D18123, doi:10.1029/2009JD013654.

Duan, Q., S. Sorooshian, and V. Gupta (1992), Effective and efficient global optimization for conceptual Rainfall-Runoff models, *Water Resour. Res.*, *28*(4), 265–284, doi:10.1029/91WR02985.

Duan, Q., N. K. Ajami, X. Gao, and S. Sorooshian (2007), Multi-model ensemble hydrologic prediction using Bayesian model averaging, *Adv. Water Resour.*, *30*, 1371–1386.

Ek, M., K. E. Mitchell, Y. Lin, E. Rogers, P. Grunmann, V. Koren, G. Gayno, and J. D. Tarpley (2003), Implementation of Noah land surface model advances in the National Centers for Environmental Prediction operational mesoscale Eta Model, *J. Geophys. Res.*, *108*(D22), 8851, doi:10.1029/2002JD003296.

Ek, M., Y. Xia, E. F. Wood, J. Sheffield, B. Cosgrove, and K. Mo (2011), The North American land data assimilation system: Application to drought over CONUS, *AGU*, Fall Meet., Abstract GC31A-1015.

Georgakakos, K. P., D. J. Seo, H. Gupta, J. Schake, and M. B. Butts (2004), Characterizing streamflow simulation uncertainty through multimodel ensembles, *J. Hydrol.*, *298*(1–4), 222–241.

Gneiting, T., A. E. Raftery, A. H. Westveld, and T. Goldman (2005), Calibrated probabilistic forecasting using ensemble model output statistics and minimum CRPS estimation, *Mon. Weather Rev.*, *133*, 1098–1118.

Hoetting, J. A., D. Madigan, A. E. Raftery, and C. T. Volinsky (1999), Bayesian modeling averaging: A tutorial, *Stat. Sci.*, *14*(4), 382–417.

Holland, J. H. (1975), *Adaptation in Natural and Artificial Systems*, 183 pp., Univ. of Michigan Press, Ann Arbor, Mich.

Hong, S., V. Lakshmi, E. E. Small, F. Chen, M. Tewari, and K. W. Manning (2009), Effects of vegetation and soil moisture on the simulated land surface processes from the coupled WRF/Noah model, *J. Geophys. Res.*, *114*, D18118, doi:10.1029/2008JD011249.

Hsu, K. L., H. Moradkhani, and S. Sorooshian (2009), A sequential Bayesian approach for hydrologic model selection and prediction, *Water Resour. Res.*, *45*, W00B12, doi:10.1029/2008WR006824.

Hupet, F., S. Lambot, M. Javaux, and M. Vanclooster (2002), On the identification of macroscopic root water uptake parameters from soil water content observations, *Water Resour. Res.*, *38*(12), 1300, doi:10.1029/2002WR001556.

Ines, A. V. M., and P. Droogers (2002), Inverse modeling in estimating soil hydraulic functions: A genetic algorithm approach, *Hydrol. Earth Syst. Sci.*, *6*(1), 49–65.

Ines, A. V. M., and B. P. Mohanty (2008), Near-surface soil moisture assimilation for quantifying effective soil hydraulic properties using genetic algorithm: I. Conceptual modeling, *Water Resour. Res.*, *44*, W06422, doi:10.1029/2007WR005990.

Ines, A. V. M., and B. P. Mohanty (2009), Near-surface soil moisture assimilation for quantifying effective soil hydraulic properties using genetic algorithm (II. Using airborne remote sensing during SGP97 and SMEX02), *Water Resour. Res.*, *45*, W01408, doi:10.1029/2008WR007022.

Jackson, T. J., M. H. Cosh, J. Famiglietti, and R. Bindlish (2009), *SMEX04 Regional Soil Moisture Data: Arizona, Digital Media*, Natl. Snow and Ice Data Cent., Boulder, Colo.

Katata, G., H. Nagai, H. Ueda, N. Agam, and P. R. Berliner (2007), Development of a land surface model including evaporation and adsorption processes in the soil for the land-air exchange in arid regions, *J. Hydrometeorol.*, *8*, doi:10.1175/2007JHM829.1.

Keefer, T., D. Goodrich, and S. Moran (2009), *SMEX04 Meteorological Network Data: Arizona*, NASA DAAC at the Natl. Snow and Ice Data Cent., Boulder, Colo.

Kennedy, J., and R. C. Eberhart (2001), *Swarm Intelligence*, Morgan Kaufmann, San Mateo, Calif.

Koren, V., J. Schaake, K. Mitchell, Q. Y. Duan, F. Chen, and J. M. Baker (1999), A parameterization of snowpack and frozen ground intended for NCEP weather and climate models, *J. Geophys. Res.*, *104*, 19,569–19,585, doi:10.1029/1999JD900232.

Koster, R., and M. Suarez (1996), Energy and water balance calculations in the Mosaic LSM, *NASA Tech. Memo. 9*, 104606.

Krishnakumar, K. (1989), *Micro-Genetic Algorithms for Stationary and Non-stationary Function Optimization*, vol. 1196, pp. 289–296, SPIE: Intelligent Control and Adaptive Systems, Philadelphia, Pa.

Kroes, J. G., J. G. Van Dam, J. Huygen, and R. W. Vervoort (1998), User's Guide of SWAP version 2.0, *Tech. Doc. 48*, DLO Winand Staring Cent., Wageningen Agric. Univ., Wageningen, Netherlands.

Krzysztofowicz, R. (1999), Bayesian theory of probabilistic forecasting via deterministic hydrologic model, *Water Resour. Res.*, *35*, 2739–2750, doi:10.1029/1999WR900099.

Krzysztofowicz, R., and K. S. Kelly (2000), Hydrologic uncertainty processor for probabilistic river stage forecasting, *Water Resour. Res.*, *36*(11), 3265–3277, doi:10.1029/2000WR900108.

Leij, F. J., W. J. Alves, M. T. van Genuchten, and J. R. Williams (1999), The UNSODA unsaturated soil hydraulic database, in *Characterization and Measurement of the Hydraulic Properties of Unsaturated Porous Media*, edited by M. T. van Genuchten et al., pp. 1269–1281, Univ. of Calif., Riverside.

Leung, L. R., M. Huang, Y. Qian, and X. Liang (2011), Climate-soil-vegetation control on groundwater table dynamics and its feedbacks in a climate model, *J. Clim.*, *36*, 57–81.

Li, H., M. Huang, M. S. Wigmosta, Y. Ke, A. M. Coleman, L. R. Leung, A. Wang, and D. M. Ricciuto (2011), Evaluating runoff simulations from the Community Land Model 4.0 using observations from flux towers and a mountainous watershed, *J. Geophys. Res.*, *116*, D24120, doi:10.1029/2011JD016276.

Liang, X., D. P. Lettenmaier, E. F. Wood, and S. J. Burges (1994), A simple hydrologically based model of land surface water, energy fluxes for general circulation models, *J. Geophys. Res.*, *99*(D7), 14,415–14,428, doi:10.1029/94JD00483.

Liu, Y., H. V. Gupta, S. Sorooshian, L. A. Bastidas, and W. J. Shuttleworth (2004), Exploring parameter sensitivities of the land surface using a locally coupled land-atmosphere model, *J. Geophys. Res.*, *109*, D21101, doi:10.1029/2004JD004730.

Liu, Y. Y., M. F. McCabe, J. P. Evans, A. I. J. M. van Dijk, R. A. M. de Jeu, and H. Su (2009), Comparison of soil moisture in GLDAS model simulations and satellite observations over the Murray Darling Basin, in *18th World IMACS Congress and MODSIM09 International Congress on Modelling and Simulation*, edited by R. S. Anderssen et al., pp. 2798–2804, Modell. and Simul. Soc. of Australia and New Zealand and Int. Assoc. for Math. and Comput. in Simul., Cairns.

MacQueen, J. (1967), Some methods for classification and analysis of multivariate observations, in *Proceedings of 5th Berkeley Symposium on Mathematical Statistics and Probability*, vol. 1, pp. 281–297, Univ. of Calif. Press, Berkeley, Calif.

Mohanty, B. P., and T. H. Skaggs (2001), Spatio-temporal evolution and time-stable characteristics of soil moisture within remote sensing footprints with varying soil, slope, and vegetation, *Adv. Water Resour.*, *24*, 1051–1067.

Mohanty, B. P., D. A. Miller, and M. T. van Genuchten (2002), Soil property database: Southern Great Plains 1997 hydrology experiment, *Water Resour. Res.*, *38*(5), 1047, doi:10.1029/2000WR000076.

Mualem, Y. (1976), A new model for predicting the hydraulic conductivity of unsaturated porous media, *Water Resour. Res.*, *12*, 513–522, doi:10.1029/WR012i003p00513.

Musters, P. A. D., W. Bouten, and J. M. Verstraten (2000), Potentials and limitations of modelling vertical distributions of root water uptake of an Austrian pine forest on a sandy soil, *Hydrol. Processes*, *14*, 103–115.

Narasimhan, B., R. Srinivasan, J. G. Arnold, and M. Di Luzio (2005), Estimation of long-term soil moisture using a distributed parameter hydrologic model and verification using remotely sensed data, *Trans. ASAE*, *48*(3), 1101–1113.

Niu, G. Y., Z. L. Yang, R. E. Dickinson, L. E. Gulden, and H. Su (2007), Development of a simple groundwater model for use in climate models and evaluation with gravity recovery and climate experiment data, *J. Geophys. Res.*, *112*, D07103, doi:10.1029/2006JD007522.

Oleson, K. W., G.-Y. Niu, Z.-L. Yang, D. M. Lawrence, P. E. Thornton, P. J. Lawrence, R. Stockli, R. E. Dickinson, G. B. Bonan, S. Levis, A. Dai, and T. Qian (2008), Improvements to the Community Land Model and their impact on the hydrological cycle, *J. Geophys. Res.*, *113*, G01021, doi:10.1029/2007JG000563.

Oleson, K. W., D. M. Lawrence, G. B. Bonan, M. G. Flanner, E. Kluzek, P. J. Lawrence, S. Levis, S. C. Swenson, and P. E. Thornton (2010), Technical description of version 4.0 of the Community Land Model (CLM), *NCAR Tech. Notes* (*NCAR/TN-478+STR*), 257 pp.

Philip, J. R., and D. de Vries (1957), Moisture movement in porous materials under temperature gradients, *Eos Trans. AGU*, *38*, 222–232.

Radell, D. B., and C. M. Rowe (2008), An observational analysis and evaluation of land surface model accuracy in the Nebraska Sand Hills, *J. Hydrometeorol.*, *9*, doi:10.1175/2007JHM913.1.

Raftery, A. E., T. Gneiting, F. Balabdaoui, and M. Polakowski (2005), Using Bayesian model averaging to calibrate forecast ensembles, *Mon. Weather Rev.*, *133*, 1155–1174.

Reed, P., B. Minsker, and D. E. Goldberg (2000), Designing a competent simple genetic algorithm for search and optimization, *Water Resour. Res.*, *36*(12), 3757–3761, doi:10.1029/2000WR900231.

Ritter, A., F. Hupet, R. Munoz-Carpena, S. Lambot, and M. Vanclooster (2003), Using inverse methods for estimating soil hydraulic properties from field data as an alternative to direct methods, *Agr. Water Manag.*, *59*, 77–96.

Rojas, R., L. Feyen, and A. Dassargues (2008), Conceptual model uncertainty in groundwater modeling: Combining generalized likelihood uncertainty estimation and Bayesian model averaging, *Water Resour. Res.*, *44*, W12418, doi:10.1029/2008WR006908.

Rosero, E., Z.-L. Yang, T. Wagener, L. E. Gulden, S. Yatheendradas, and G.-Y. Niu (2010), Quantifying parameter sensitivity, interaction, and transferability in hydrologically enhanced versions of the Noah land surface model over transition zones during the warm season, *J. Geophys. Res.*, *115*, D03106, doi:10.1029/2009JD012035.

Sahoo, A. K., P. A. Dirmeyer, P. R. Houser, and M. Kafatos (2008), A study of land surface processes using land surface models over the Little River Experimental Watershed, Georgia, *J. Geophys. Res.*, *113*, D20121, doi:10.1029/2007JD009671.

Schaap, M. G., F. J. Leij, and M. T. van Genuchten (1999), A bootstrap-neural network approach to predict soil hydraulic parameters, in *Proc. Int. Workshop, Characterization and Measurements of the Hydraulic Properties of Unsaturated Porous Media*, edited by M. T. van Genuchten, F. J. Leij, and L. Wu, pp. 1237–1250, Univ. of Calif., Riverside.

Shin, Y., and B. P. Mohanty (2013), Development of a deterministic downscaling algorithm for remote sensing soil moisture footprint using soil and vegetation classifications, *Water Resour. Res.*, *49*, 6208–6228, doi:10.1002/wrcr.20495.

Shin Y., B. P. Mohanty, and A. V. M. Ines (2012), Soil hydraulic properties in one-dimensional layered soil profile using layer-specific soil moisture assimilation scheme, *Water Resour. Res.*, *48*, W06529, doi:10.1029/2010WR009581.

Shin, Y., B. P. Mohanty, and A. V. M. Ines (2013), Estimating effective soil hydraulic properties using spatially distributed soil moisture and evapotranspiration products at multiple scales, *Vadose Zone J.*, *12*, doi:10.2136/vzj2012.0074.

Sloughter, J. M., A. E. Raftery, and T. Gneiting (2006), Probabilistic quantitative precipitation forecasting using Bayesian model averaging, *Tech. Rep. 496*, Dep. of Stat., Univ. of Washington, Seattle.

Sridhar, V., R. L. Elliott, F. Chen, and J. A. Brotzge (2002), Validation of the NOAH-OSU land surface model using surface flux measurements in Oklahoma, *J. Geophys. Res.*, *107*(D20), 4418, doi:10.1029/2001JD001306.

Todini, E. (2008), A model conditional processor to assess predictive uncertainty in flood forecasting, *Intl. J. River Basin Manag.*, *6*(2), 123–137.

Tsai, F. T.-C., and X. Li (2008), Groundwater inverse modeling for hydraulic conductivity estimation using Bayesian model averaging and variance window, *Water Resour. Res.*, *44*, W09434, doi:10.1029/2007WR006576.

Van Dam, J. C., J. Huygen, J. G. Wesseling, R. A. Feddes, P. Kabat, P. E. V. Van Waslum, P. Groenendjik, and C. A. van Diepen (1997), Theory of SWAP version 2.0: Simulation of water flow and plant growth in the soil-water-atmosphere-plant environment, *Tech. Doc. 45*, DLO Winand Staring Cent., Wageningen Agric. Univ., Wageningen, Netherlands.

Van Genuchten, M. T. (1980), A closed-form equation foe predicting the hydraulic conductivity of unsaturated soils, *Soil Sci. Soc. Am. J.*, *44*, 892–898.

Vrugt, J. A., and B. Robinson (2007), Treatment of uncertainty using ensemble methods: Comparison of sequential data assimilation and Bayesian model averaging, *Water Resour. Res.*, *43*, W01411, doi:10.1029/2005WR004838.

Vrugt, J. A., ter Braak, C. J. F., Clark, M. P., Hyman, J. M., and Robinson, B. A. (2008), Treatment of input uncertainty in hydrologic modeling: Doing hydrology backward with Markov chain Monte Carlo simulation, *Water Resour. Res.*, *44*, W00B09, doi:10.1029/2007WR006720.

Vrugt, J. A., C. J. F. ter Braak, C. G. H. Diks, B. A. Robinson, J. M. Hyman, and D. Higdon (2009), Accelerating Markov Chain Monte Carlo simulation by differential evolution with self-adaptive randomized subspace sampling, *Int. J. Nonlinear Sci. Numer. Simul.*, *10*(3), 271–288.

Wöhling, T., and J. A. Vrugt (2008), Combining multiobjective optimization and Bayesian model averaging to calibrate forecast ensembles of soil hydraulic models, *Water Resour. Res.*, *44*, W12432, doi:10.1029/2008WR007154.

Wösten, J. H. M., G. H. Veerman, and J. Stolte (1994), Water retention and hydraulic conductivity functions of top- and subsoils in the Netherlands: The staring series, *Tech. Doc. 18*, Winand Staring Centre, Wageningen, Netherlands, 66.

Wu, H., X. Zhang, S. Liang, H. Yang, and G. Zhou (2012), Estimation of clear-sky land surface longwave radiation from MODIS data products by merging multiple models, *J. Geophys. Res.*, *117*, D22107, doi:10.1029/2012JD017567.

Ying, M., S. Feng, Z. Huo, and X. Song (2011), Application of the SWAP model to simulate the field water cycle under deficit irrigation in Beijing, China, *Math. Comput. Model.*, *54*, 1044–1052.

Zeng, X. B., and M. Decker (2009), Improving the numerical solution of soil moisture-based Richards equation for land models with a deep or shallow water table, *J. Hydrometeorol.*, *10*, 308–319.

Zhang, X., R. Srinivasan, K. Zhao, and M. V. Liew (2008), Evaluation of global optimization algorithms for parameter calibration of a computationally intensive hydrologic model, *Hydrol. Processes*, doi:10.1002/hyp.7152.

Zhang, X., R. Srinivasan, and D. Bosch (2009), Calibration and uncertainty analysis of the SWAT model using Genetic Algorithms and Bayesian Model Averaging, *J. Hydrol.*, *374*, 307–317.

Zhu, J., and B. P. Mohanty (2006), Effective scaling factor for transient infiltration in heterogeneous soils, *J. Hydrol.*, *319*, 96–108.